iScience

CellPress
OPEN ACCESS

Article

# *Leishmania amazonensis* sabotages host cell SUMOylation for intracellular survival

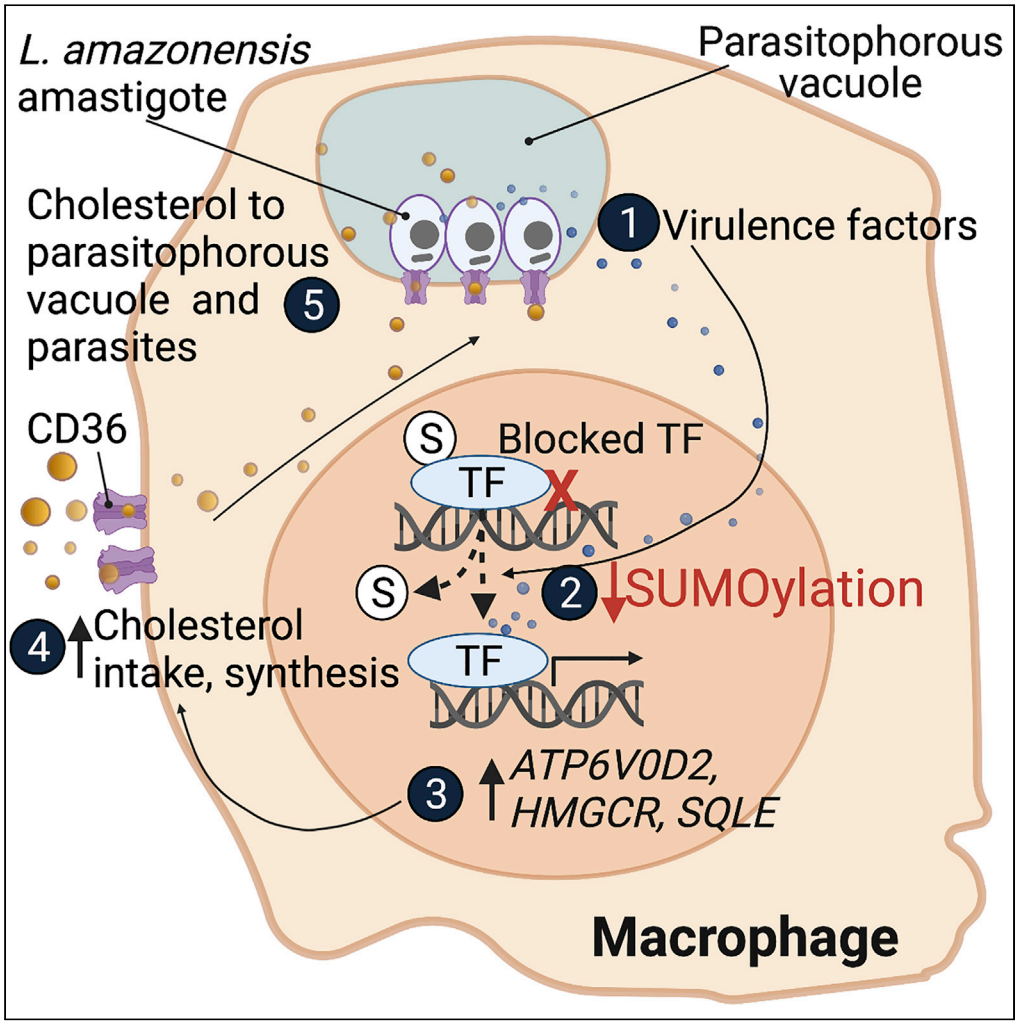


Kendi Okuda, Miriam Maria Silva Costa Franco, Ari Yasunaga, Ricardo Gazzinelli, Michel Rabinovitch, Sara Cherry, Neal Silverman

cherrys@pennmedicine.upenn.edu (S.C.)
neal.silverman@umassmed.edu (N.S.)

## Highlights

*Drosophila* used as discovery platform to probe *Leishmania*-macrophage interactions

In mammalian macrophages, amastigotes potently inhibit protein SUMOylation

Inhibition of SUMOylation favors amastigote proliferation within macrophages

*ATP6V0D2* expression and cholesterol levels increase to support amastigote growth

Okuda et al., iScience *25*, 104909
September 16, 2022 
https://doi.org/10.1016/j.isci.2022.104909

iScience

CellPress
OPEN ACCESS

Article

# *Leishmania amazonensis* sabotages host cell SUMOylation for intracellular survival

Kendi Okuda,[1] Miriam Maria Silva Costa Franco,[1] Ari Yasunaga,[2] Ricardo Gazzinelli,[1,3,4] Michel Rabinovitch,[5] Sara Cherry,[2,*] and Neal Silverman[1,6,*]

## SUMMARY

***Leishmania* parasites use elaborate virulence mechanisms to invade and thrive in macrophages. These virulence mechanisms inhibit host cell defense responses and generate a specialized replicative niche, the parasitophorous vacuole. In this work, we performed a genome-wide RNAi screen in *Drosophila* macrophage-like cells to identify the host factors necessary for *Leishmania amazonensis* infection. This screen identified 52 conserved genes required specifically for parasite entry, including several components of the SUMOylation machinery. Further studies in mammalian macrophages found that *L. amazonensis* infection inhibited SUMOylation within infected macrophages and this inhibition enhanced parasitophorous vacuole growth and parasite proliferation through modulation of multiple genes especially *ATP6V0D2*, which in turn affects *CD36* expression and cholesterol levels. Together, these data suggest that parasites actively sabotage host SUMOylation and alter host transcription to improve their intracellular niche and enhance their replication.**

## INTRODUCTION

*Leishmania* parasites use multiple strategies to thrive in mammalian phagocytes. One striking example is the use of virulence factors to evade or down regulate the host immune response. For example, amastigote forms of the parasite invade macrophages, and express surface molecules that engage phagocytic receptors that promote 'silent' or anti-inflammatory cell invasion, typically observed with the engulfment of apoptotic cells (Guy and Belosevic, 1993; Love et al., 1998; Peters et al., 1995; Wanderley et al., 2009, 2012). Inside macrophages, amastigotes live within specialized replicative organelles known as parasitophorous vacuoles (PVs), which are modified mature phagosomes. Amastigotes create a hospitable niche in the PV through secretion of virulence factors that dampen host cell defenses. These secreted factors work through many mechanisms including altering host protein expression and modulating post-translational protein modifications (Cameron et al., 2004; Contreras et al., 2010; deAraujo Soares et al., 2003; Halle et al., 2009; Isnard et al., 2012; Kima, 2014; reviewed in Mottram et al., 2004; Olivier et al., 2005). In particular, species in the *Leishmania mexicana* group (including *Leishmania amazonensis*) promote the biogenesis of super enlarged PV which is thought to be essential to parasite persistence in the infected tissues and to cause cutaneous leishmaniasis. Our understanding of the virulence mechanisms used by these parasites is incomplete while a deeper understanding is essential to develop new strategies to combat leishmaniasis, which threatens 12 million people (Alvar et al., 2012).

Mammalian models of *Leishmania* infection have been essential to build our current understanding of leishmaniasis. However, other models of infection, such as *Drosophila melanogaster,* are attractive alternatives because they share many key signaling pathways with mammals and have powerful genetic and genomic techniques readily accessible. Here, we exploited the *Drosophila* SL2 macrophage-like cell line in a genome-wide RNAi screen to identify host factors required for *L. amazonensis* infection. With this screen, we identified and validated 52 conserved host factors specifically involved in *L. amazonensis* entry but not *Escherichia coli* nor *Staphylococcus aureus* phagocytosis. These hits were particularly enriched in SUMOylation factors.

SUMOylation is a ubiquitous post-translational modification in which a Small Ubiquitin-like MOdifier protein (SUMO) is conjugated to lysine (Lys) residues on target proteins, through the sequential action of E1 activating (Sae1/Uba2 dimer), E2 conjugating (Ubc9) and E3 ligases (several of them) enzymes (Flotho and

[1]Division of Infectious Diseases and Immunology, Department of Medicine, University of Massachusetts Medical School, Worcester, USA

[2]Department of Microbiology, University of Pennsylvania, Philadelphia, PA, USA

[3]Centro de Tecnologia de Vacinas, Universidade Federal de Minas Gerais, Belo Horizonte, MG 31270, Brazil

[4]Fundação Oswaldo Cruz - Minas, Belo Horizonte, MG 30190, Brazil

[5]Department of Microbiology, Immunology and Parasitology, Escola Paulista de Medicina, Universidade Federal de São Paulo, São Paulo, Brazil

[6]Lead contact

*Correspondence: cherrys@pennmedicine.upenn.edu (S.C.), neal.silverman@umassmed.edu (N.S.)

https://doi.org/10.1016/j.isci.2022.104909

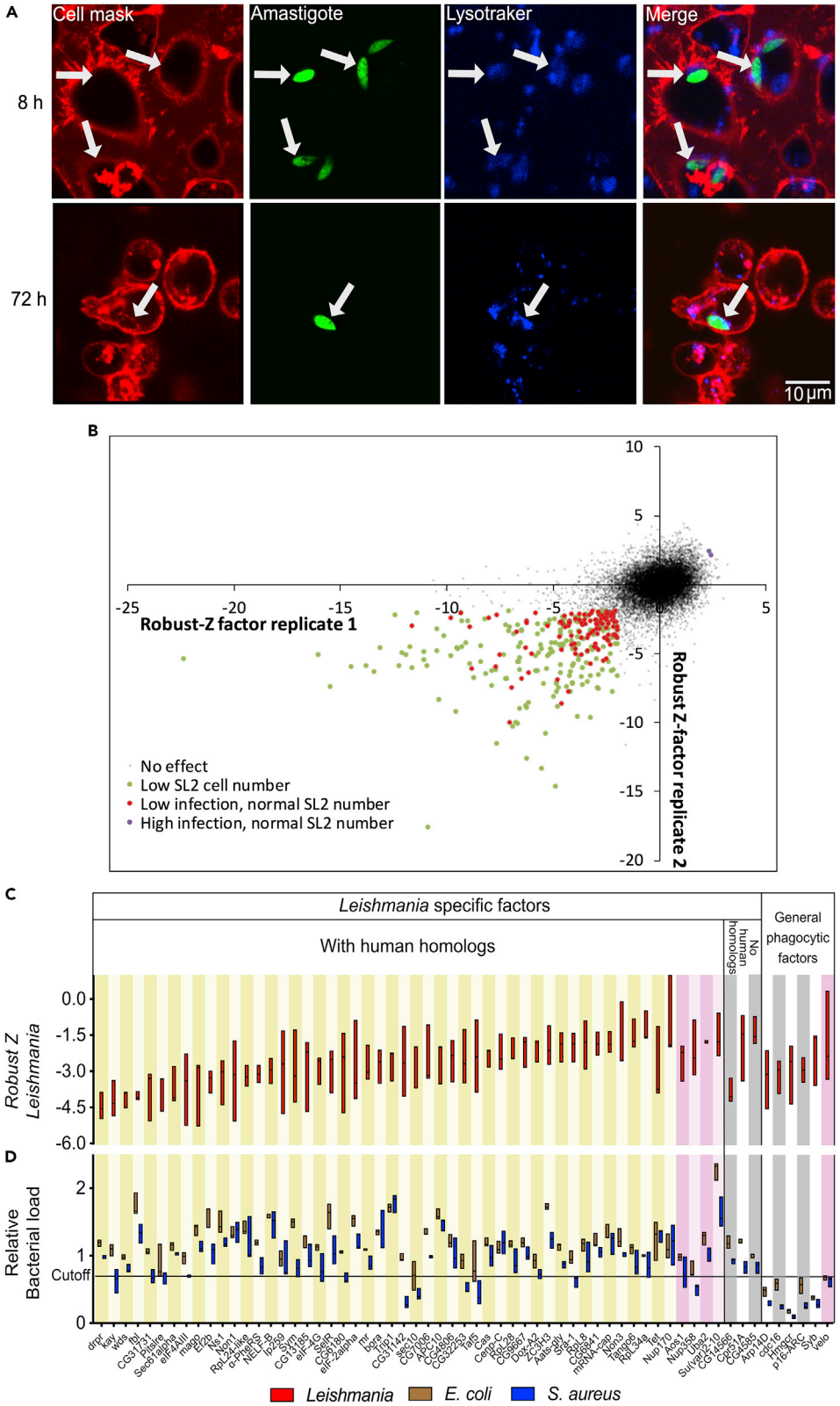
A
Cell mask
Amastigote
Lysotraker
Merge
8 h
72 h
10 µm
B
Robust-Z factor replicate 1
Robust Z-factor replicate 2
No effect
Low SL2 cell number
Low infection, normal SL2 number
High infection, normal SL2 number
C
Leishmania specific factors
With human homologs
No human homologs
General phagocytic factors
Robust Z Leishmania
D
Relative Bacterial load
Cutoff
Leishmania
E. coli
S. aureus

**Figure 1. Genome-wide high-throughput RNAi screen of amastigote internalization**

A) *L. amazonensis* amastigotes enter *Drosophila* SL2 cells. Confocal microscopy of SL2 cells infected with GFP expressing amastigotes (arrows). Acidic compartments were stained with Lysotracker (blue) and the cell membrane with Cellmask (red).

(A) At 8 h of infection, intracellular amastigotes (green) are contained in small phagosomes lighly stained with lysotracker. By 72 h PVs are still small but now rich in Lysotracker. Images representative of 2 independent experiments.

(B) *Drosophila* SL2 cells were transfected with dsRNAs representing the entire genome (~13,000 dsRNA) and screened in biologically independent duplicates. The level of infection was quantified as presented in Figures S1 and S2, using automated microscopy. Although most knockdowns did not cause a reproducible and significant change in the infection rate (gray dots), 118 knockdowns reduced the infection in both replicates, but did not affect cell proliferation (red dots), whereas 2 increased parasite uptake in both replicates without affecting proliferation (purple dots). Potential hits that also affected SL2 cell proliferation are marked with green dots (195 in total).

(C and D) 61 hits were validated with independent dsRNAs and then examined for their effect on the internalization of *E. coli* and *S. aureus* particles. The top part of the graph shows the *Leishmania* infection Z-scores of triplicate validation assays whereas the bottom portion shows the results with bacterial internalization assays using flow cytometry in triplicates. The cutoff for reduced bacterial internalization was set to a median value of 30% below the median of 6 replicates of the control non-targeting GFP RNAi. This cutoff represents an average of 3 standard deviations below the mean. Six candidates decreased phagocytosis of these two bacteria as well as *Leishmania,* and are likely generally involved in phagocytosis. Results from 3 independent experiments, with the measurement of 20,000 events per sample. The final list of *Leishmania* specific hits is composed of 52 genes with human homologs displayed on the left side of the Figure 1D. SUMOylation factors are highlighted in light and dark pink and the three *Drosophila* genes with no human homologs are indicated.

Melchior, 2013). SUMOylation regulates gene expression, protein function, localization or activity (Gill, 2004), and 6,747 different SUMOylated proteins were cataloged in HeLa and U2OS cell lines (Hendriks et al., 2017).

Of interest, many pathogens, including virus, bacteria and protozoans, target SUMOylation to exploit host cellular functions or to inhibit cell defense responses (Fritah et al., 2014; Lowrey et al., 2017; Mohapatra et al., 2019; Orth et al., 2000; Ribet et al., 2010; Verma et al., 2015). Here, we observed that intracellular *L. amazonensis* amastigotes efficiently inhibited overall macrophage SUMOylation, reducing this post-translational modification to nearly undetectable levels. Moreover, SUMO1 or SUMO2 depleted cells presented enhanced parasite growth with larger PVs, higher expression of *ATP6V0D2,* and consequently elevated *CD36* and cholesterol levels. Therefore, our data suggest that inhibition of SUMOylation is a novel virulence mechanism of *L. amazonensis* parasites, used for successful infection of macrophages.

## RESULTS

### The *Drosophila* cell model of *L. amazonensis* infection

*Drosophila* macrophages, also known as plasmatocytes, play key roles in immune defense and development (Gold and Bruckner, 2015). Previously, we demonstrated that these macrophages use CD36-like scavenger receptors to phagocytose and control proliferation of *L. amazonensis* in the hemolymph of adult flies (Okuda et al., 2016). In this work, we determined if the *Drosophila* macrophage-like SL2 cell line would phagocytose parasites, in particular the amastigote form that is responsible for repeated cycles of macrophage infections in mammalian hosts. Throughout this work we used antibody-free, intracellular amastigotes harvested from infected BMDM cultures. In culture, *L. amazonensis* amastigotes were promptly phagocytosed and observed within SL2 cells (Figure 1A, 8 h). By 72 h after infection, parasites were inside small acidic (LysoTracker positive) vacuoles (Figure 1A 72 h), and by 96 h after infection intracellular parasites were mostly cleared from these cells (not shown).

As PV biogenesis and parasite proliferation were not observed in the SL2 cell model, our initial focus was on the phagocytosis and entry of amastigotes, a step that is essential for leishmaniasis development. To quantify intracellular parasites, SL2 cells were infected with GFP-expressing amastigotes, fixed and extracellular parasites were immunostained with anti-*Leishmania* serum. The ratio of intracellular parasites (immunostaining negative) and SL2 cell number (Hoechst 33,342 stain of nucleus) was scored microscopically using image analysis software (see Figures S1A and S1B). The phagocytosis of parasites increased over the 4-h time course of this assay, with ~70% of the internalization completed by 90 min using a multiplicities of infection (MOI) equal to 2 (see Figure S1C). The effect of several MOIs was analyzed at 90 min post infection (pi). Although the percentage of infected cells and the number of internalized parasites increased with higher MOI (see Figures S1D–S1F), the number of cells containing two or more parasites also increased

(see Figures S1G and S1E). Reliable and accurate automated quantification of individual parasites is difficult when two or more parasites are in the same cell due their closeness. Therefore, we selected a MOI of 0.5 for 90 min for screening where we observed 80% of infected cells have one intracellular parasite and 17% have two (Figure S1G). We tested the robustness of the assay by infecting and scoring 24 replicate wells, either with no RNAi, or transfected with RNAi control without a target gene (non-silencing), or targeting genes known to be required for phagocytosis (βCOP, Cdc42) (Hackam et al., 2001; Morehead et al., 2002; Okuda et al., 2016; Peltan et al., 2012; Ramet et al., 2002) (see Figures S2A–S2C). These phagocytosis genes clearly and significantly reduced amastigote entry.

We then used this assay to identify factors required for the internalization of *L. amazonensis* into SL2 cells by performing a genome-wide RNAi screen with a library of 13,071 dsRNAs covering nearly the entire *Drosophila* genome (Ambion). For each knockdown, four microscopic fields with approximately 1,000 cells each were imaged. The number of intracellular parasites per cell for each RNAi treatment was quantified and the Robust Z-score was calculated (the distance of the infection in each well from the median of the entire 384 well plate) (Zhang et al., 2006).

The entire library was screened in two completely independent replicates and the Z-scores of infection from the duplicate screens are presented in the Figure 1C, where X- and Yaxes display the Z-scores of each replicate, and each dot represents a distinct RNAi treatment (the complete dataset of preliminary hits is also presented in Table S1). We used a cutoff of- $\leq$ -2.0 or $\geq$2 in both replicates ($p<0.001$) to identify the genes potentially required for parasite entry, and genes that potentially restrict entry (referred to as 'down' and 'up' hits hereafter). Further, those candidates that reduced SL2 cell viability and/or proliferation (Z-score of cell number $\leq$-2.0 in both samples, green dots in Figure 1B) were removed from further analysis. This analysis revealed 120 candidate genes (118 downs and 2 up hits, red and purple dots in Figure 1B). Independent dsRNAs targeting these candidates, free of predicted off-targets (Hu et al., 2017), were synthesized and used in validation assays performed in triplicate. This secondary screen validated 61 down hits but neither of the initial candidate ups (Figure 1C and Table S1).

Among these 61 down hits, we next sought to determine which generally impact phagocytosis and which are specifically required for uptake of *Leishmania* amastigotes. To this end, we performed phagocytosis assays with FITC-labeled *E. coli* and *S. aureus* (Wan et al., 1993). We quantified uptake of FITC labeled *E. coli* and *S. aureus* using flow cytometry (Ramet et al., 2002). Six candidates reduced the internalization of both *E. coli* and *S. aureus* by $\geq$30% and were thus classified as general phagocytic factors, whereas 55 were more specific to *Leishmania* (Figure 1D and Table S1). Three of the *Leishmania* specific hits have no clear human homologs, leaving 52 down hits for further investigations.

## *Leishmania* uptake factors are highly enriched in protein SUMOylation

In order to identify host cell biological processes affected by the 52 conserved hits from our genome-wide RNA screen, these candidates were submitted to an overrepresentation test using Panther, with the *Drosophila* GO-Slim biological process network (Mi et al., 2019). "Protein SUMOylation" was 91-fold enriched with a P-value of 5.04E-03 (see Table 1). Three of the thirteen genes that make up the protein SUMOylation group were hits - both SUMO E1 subunit genes *Aos1* and *Uba2*, as well as the SUMO E3 ligase, *Su(var)2–10* (aka PIAS). In addition, the single *Drosophila* SUMO ortholog *smt3* reduced infection, but also affected cell proliferation, whereas the SUMO protease *velo* (SENP6/7 homolog) affected both *Leishmania* entry and bacterial phagocytosis (Figures 1C and 1D marked with pink stripes, and Table S1).

## *L. amazonensis* drastically reduces macrophage SUMOylation

We next set out to define a role for protein SUMOylation in infection of mammalian macrophages using antibody-free amastigotes harvested from mouse bone marrow-derived macrophages (BMDM). We infected naive BMDMs with *L. amazonensis* amastigotes and harvested whole cell lysates at various time points after infection; total protein SUMOylation was analyzed by immunoblotting for SUMO1 or SUMO2/3 (Figures 2A and 2B). Uninfected macrophages presented numerous SUMO-conjugated bands ranging from ~60 to >250 kDa. This overall SUMOylation signal visibly decreased 2 h after *L. amazonensis* amastigote infection and was nearly undetectable by 48 h after infection, with either SUMO1 or SUMO2/3 probes. The infection did not change the quantity of free SUMO2/3 bands (Figure 2B, 15 kDa band), free SUMO1 was not detectable. This loss of SUMOylation was not due to total protein

**Table 1. *Leishmania*-specific hits are enriched in SUMOylation factors**

| GO-Slim Biological Process | Total genes | Number of hits | Fold enrichment | Raw p value | Hits | FDR |
|---|---|---|---|---|---|---|
| Protein SUMOylation | 13 | 3 | 91.13 | 3.40E-05 | Uba2, Aos1, Su(var)2–10 | 5.04E-03 |
| Ribosomal large subunit biogenesis | 46 | 3 | 25.75 | 4.60E+01 | Non1, Non3, lp259 | 4.70E-02 |
| Gene expression | 1479 | 12 | 3.2 | 7.10E-03 | cas, Sra-1, Tet, Non3, RpL8, mRNA-cap, Su(var)2–10, Raf5, Sec61alpha, lp259, mago, *sym* | 3.75E-02 |
| Cellular nitrogen compound metabolic process | 1807 | 13 | 2.84 | 2.94E-04 | cas, Tet, Sra-1, Non3, RpL8, mRNA-cap, Su(var)2–10, fbl, Taf5, Sec61alpha, lp259, mago, Sym | 4.99E-02 |

Panther GO-Slim biological process analysis of the 52 *Drosophila* genes revealed significant enrichment for SUMOylation, Ribosomal large subunit assembly, gene expression and cellular nitrogen compound metabolic process. Overrepresentation test for biological process using Panther, with the *Drosophila* GO network. "Total genes #" are the number of genes contained in the GO term, whereas "From input#" is the number of hits found in the GO term, "Fold Enrichment" is the fold increase of found genes relative to the expected number of genes, "raw p value" is the statistical significance of enrichment, whereas "FDR" is the false discovery rate.

degradation or sample loading issues, as normal levels total protein were observed by Coomassie Blue staining of the same membrane after immunoblotting (Figure 2 at the bottom of each blot).

The sandfly bite transmits the promastigote form of the parasite to the human skin, where they infect phagocytes by receptor mediated phagocytosis (Ueno and Wilson, 2012). Once internalized, promastigotes differentiate into amastigotes, a differentiation process that typical requires 48–72 h (Courret et al., 2001). Of interest, BMDM infection with promastigotes caused a delayed reduction of SUMO1 and SUMO2/3 conjugation, which was observed only after 48 h of infection (Figures 2A and 2B, middle). This delayed inhibition of SUMOylation with promastigote infection correlates with the time required for differentiation of promastigote into amastigotes (Courret et al., 2001). On the other hand, phagocytosis of heat-killed amastigotes did not substantially change SUMO1 or SUMO2/3 signal, besides a slightly reduced SUMO1ylation signal at 24 h (Figures 2A and 2B, right). All together, these data argue that live intracellular amastigotes, but not promastigotes, are potent inhibitors of overall macrophage protein SUMOylation.

To determine if similar regulation of SUMOylation occurs in human systems, THP-1 macrophages (Mehta et al., 2010) were similarly analyzed following amastigote infection. The infection of these human macrophages with amastigotes drastically reduced overall levels of protein SUMO2/3-ylation with little or no change in free SUMO2/3 (Figure 2C). The overall protein SUMO2/3ylation was at undetectable levels at 72 h after infection. In addition, a THP-1 cell line was generated that constitutively over-expresses HA-SUMO2, which exhibited increased levels of free SUMO2 as well as SUMOylated proteins in uninfected cells (Figure 2C). Although the loss of SUMOylation was delayed in this case, parasite infection still reduced it to undetectable levels by 72 h after infection.

Next, we investigated if the intracellular parasites were able to inhibit protein SUMOylation induced by heat shock, a classic inducer of elevated SUMOylation (Seifert et al., 2015). BMDMs were first infected with amastigotes for various times, and then were heat shocked at 43°C for 30 min. Similar to observations in the human lymphoblast cell line K-562 (Niskanen et al., 2015), heat shock induced the SUMOylation of high molecular weight proteins in uninfected BMDMs (Figure 2D, NI). However, this SUMOylation was strongly inhibited in cells infected with amastigotes for 2 h, 8 h or 24 h (Figure 2D), indicating that *Leishmania* parasites actively suppress SUMOylation induced by external stimuli.

One possibility is that virulence factors produced by intracellular amastigotes actively reduce the pool of macrophage SUMOylated proteins. To investigate this hypothesis we studied, by Western blot, the presence of E1 and E2 SUMO enzymes. In mammals, although many E3 ligases are involved in protein SUMOylation, there is only one E1 enzyme formed by SAE1 and SAE2 heterodimers and only one E2 enzyme (UBC9) and therefore E1 and E2 enzymes is a strategic target for SUMOylation inhibition in bacteria and parasites (Fritah et al., 2014; Maruthi et al., 2017; Ribet et al., 2010; Sidik et al., 2015). Western blots with antibodies against SAE1 (E1) or UBC9 (E2) demonstrate that these enzymes are present in comparable

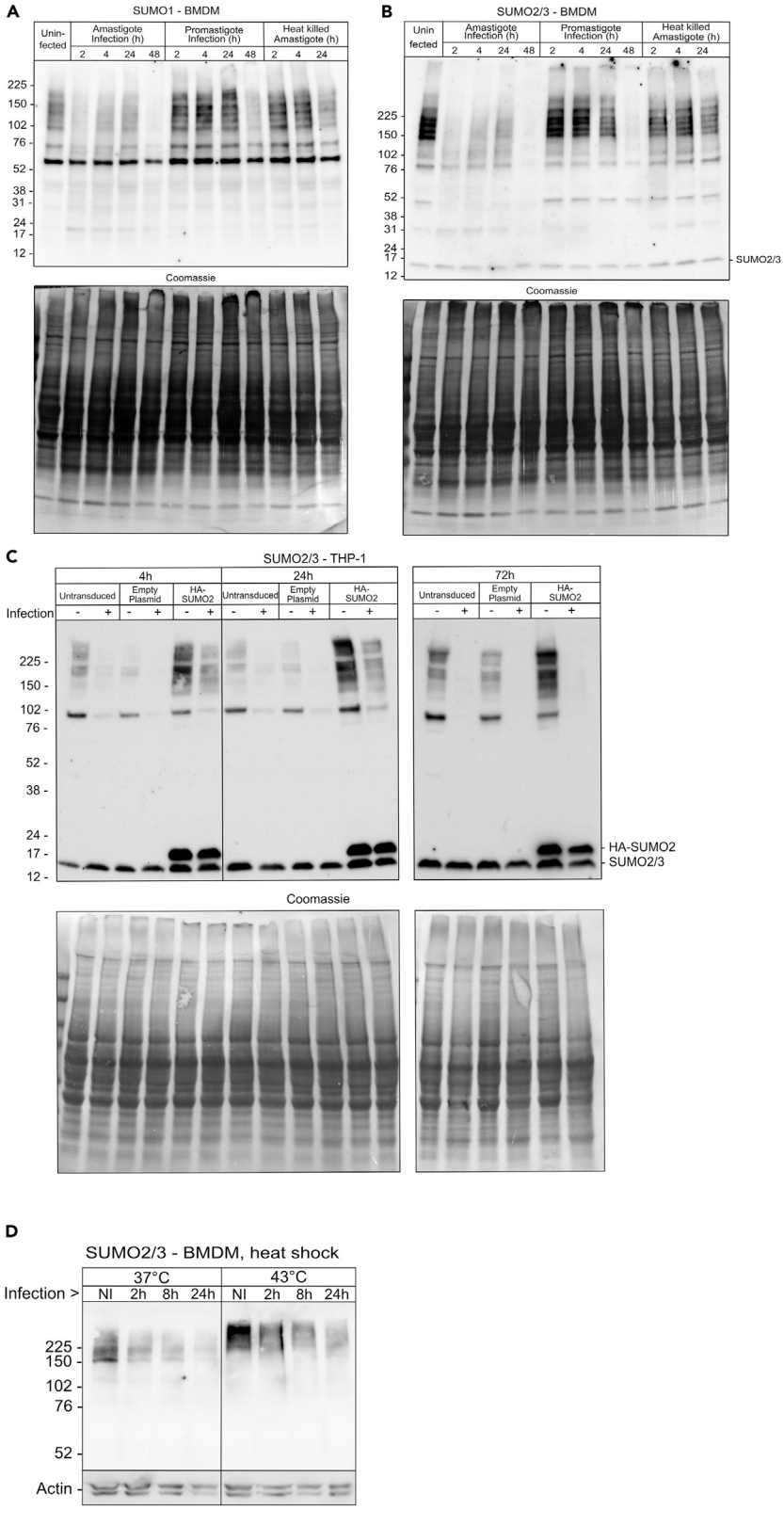
A
SUMO1 - BMDM
Unin-fected
Amastigote Infection (h)
Promastigote Infection (h)
Heat killed Amastigote (h)
2 4 24 48 2 4 24 48 2 4 24
225
150
102
76
52
38
31
24
17
12
Coomassie
B
SUMO2/3 - BMDM
Unin fected
Amastigote Infection (h)
Promastigote Infection (h)
Heat killed Amastigote (h)
2 4 24 48 2 4 24 48 2 4 24
225
150
102
76
52
38
31
24
17
12
SUMO2/3
Coomassie
C
SUMO2/3 - THP-1
4h
24h
72h
Untransduced
Empty Plasmid
HA-SUMO2
Infection
- + - + - + - + - + - + - + - +
225
150
102
76
52
38
24
17
12
HA-SUMO2
SUMO2/3
Coomassie
D
SUMO2/3 - BMDM, heat shock
37°C
43°C
Infection >
NI 2h 8h 24h NI 2h 8h 24h
225
150
102
76
52
Actin

**Figure 2. *Leishmania* amastigote infection reduces SUMOylation in mouse and human macrophages**

Macrophages (A and B - mouse BMDM, C - THP-1 human macrophages) were infected with amastigotes (MOI of 5) or promastigotes (MOI of 10), and at indicated times cells were lysed, separated by SDS-PAGE and analyzed by immunoblotting for SUMO1 (A) or SUMO2/3 (B, C). Reduction of SUMO1 and SUMO2/3 SUMOylation is noticeable starting at 2 h after infection of BMDM and a even strong at 48 h after infection with amastigotes. Infection initiated with promastigotes initially presented a modest increase in SUMO1-ylation, followed by reduction in SUMO1 or SUMO2/3-ylation at 48 h, corresponding to the time required for the differentiation of promastigotes into amastigotes. Heat killed amastigotes only slightly reduced SUMO1ylation at 24 h but in general did not markedly change the SUMO signal.

(C) Similarly, in THP-1 macrophages amastigote infection (MOI = 5) reduced SUMO2/3ylation up to 72 h when SUMOylated proteins were no longer detected. Expression of HA-SUMO2 increases the overall amount of SUMOylated proteins and delays, but does not prevent, the deSUMOylation caused by infection. The total protein levels are similar by Coomassie Blue staining showed below each immunoblot.

(D) Amastigote infection inhibits SUMOylation induced by heat shock. After infection for the indicated times, cells were heat shocked at 43°C for 30 min to induce SUMOylation and analyzed by immunoblotting for SUMO2/3. Heat shock induced a strong SUMOylation of high molecular weight proteins in non-infected cells (NI) and only slightly in infected cells. Anti-actin loading control shows comparable signals in each sample. Representative results of 3 independent experiments.

levels in uninfected and macrophages infected for 2 h, 8 h and 24 h (see Figure S3). Therefore, intracellular amastigotes do not degrade SUMOylation enzymes to block macrophage protein SUMOylation and the mechanism is still unclear.

## SUMOylation inhibition favors *Leishmania* infection

Several pathogens sabotage the SUMOylation machinery to better survive in the vertebrate host (Maruthi et al., 2017; Ribet and Cossart, 2018; Wilson, 2017). We hypothesized that protein SUMOylation attenuates amastigote proliferation, and the inhibition of SUMOylation by *Leishmania* amastigotes could be a virulence mechanism to enhance their survival or replication within macrophages. To evaluate this hypothesis, THP-1 cells were transduced with lentivirus stably expressing shRNAs specifically targeting SUMO1 or SUMO2. The efficiency of knockdowns was approximately 50%, determined by qRT-PCR (Figure 3A). The SUMO1 knockdown specifically reduced the SUMO1 protein SUMOylation whereas SUMO2 knockdown reduced the signal of higher molecular weight proteins conjugated with both SUMO1 and SUMO2/3 (Figure 3B). Unlike the *Drosophila* screen results, where knockdown of SUMOylation factors reduced amastigote uptake, in THP-1 macrophages the initial number of parasites per cell was not significantly affected, indicating amastigote entry was unaffected (Figure 3C, 6 h after infection). However, by 96 h the number of parasites per 100 macrophages was significantly higher in SUMO1 and SUMO2 knock down cells compared to the control cells (Figure 3C). Because the initial parasite uptake can affect the final number of parasites at 96 h we also calculated the increase of parasite loads at 96 h relative to initial of infection and we observed that amastigotes proliferate more in SUMO depleted cells (Figure 3D). Importantly, THP-1 macrophages overexpressing SUMO2, which partially recovered SUMOylated proteins (Figure 2C), presented significantly lower absolute parasite loads at 96 h after infection and lower proliferation, when compared to initial infection loads (Figures 3E and 3F). These findings are consistent with our hypothesis that SUMO-dependent process interfere with amastigote growth and argue that amastigotes strongly restrain macrophage SUMOylation to enhance their intracellular niche and increase parasite growth.

## SUMOylation inhibition promotes PV enlargement, drives *ATP6V0D2* expression and cholesterol retention

Intracellular amastigotes from the *L. mexicana* group, including *L. amazonensis* induce the biogenesis of enlarged PVs, which favor their survival and replication. We investigated the hypothesis that reduction of SUMOylation could promote PV biogenesis. Indeed, macrophages with knockdown of SUMO1 or SUMO2 presented larger PVs than control cells (Figures 3G and 3H), consistent with the hypothesis that disruption of macrophage SUMOylation enhances parasite growth and favors PV maturation.

The mechanisms driving the PV biogenesis are of great interest but still poorly understood. In our previous work we demonstrated that the scavenger receptor CD36 participates in the biogenesis of *L. amazonensis* PV whereas Pessoa et al. (2019) reported that an alternate subunit of the V-ATPase, Atp6v0d2, is involved in PV enlargement and parasite survival by regulating *CD36* expression and cholesterol retention (Pessoa et al., 2019). Thus, we investigated if SUMOylation inhibition promotes cholesterol retention and/or the expression of *ATP6V0D2*, *CD36*.

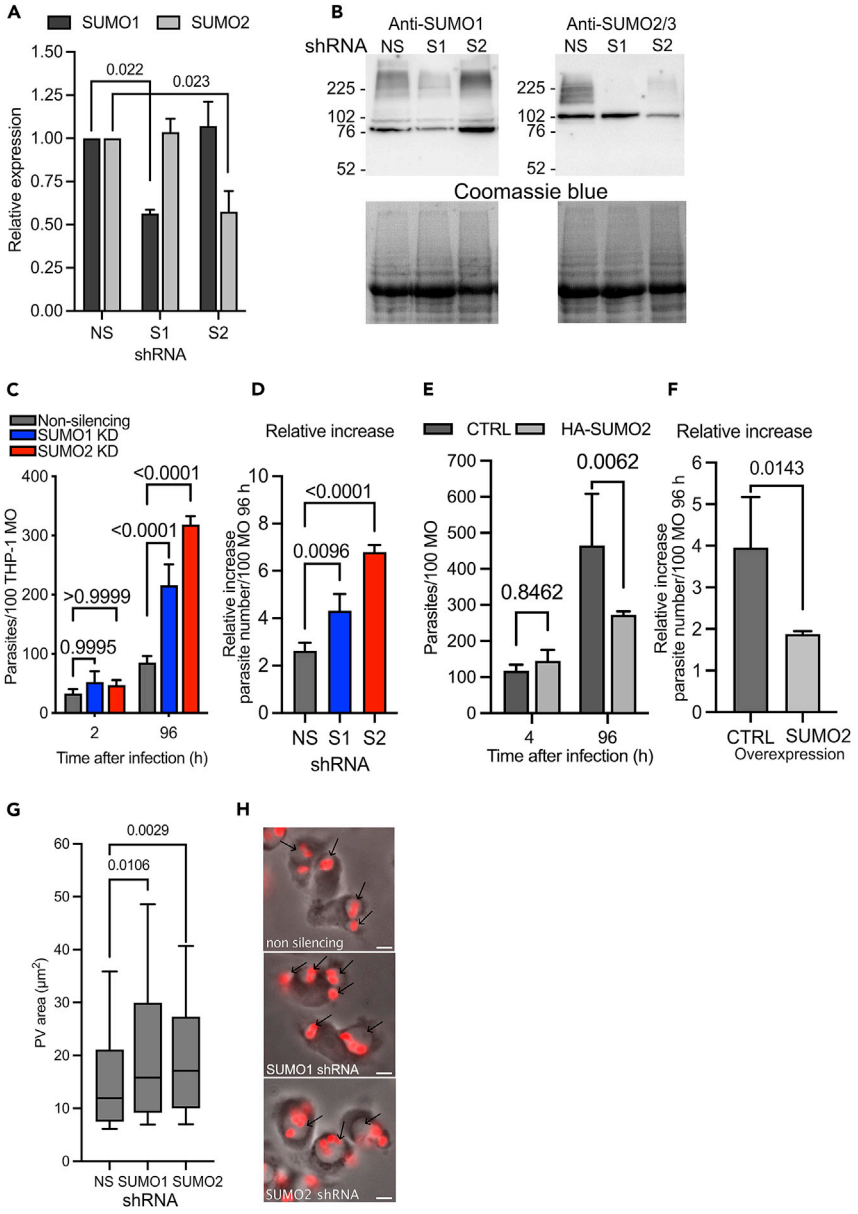


**Figure 3. Host SUMOylation modulates *L. amazonensis* infection**

THP-1 cells were transduced with lentivirus expressing non-silencing (NS) shRNA or against SUMO1 (S1) or SUMO2 (S2) and differentiated to macrophages using PMA.

(A) Efficiency of SUMO1 or SUMO2 knockdown measured by qRT-PCR. N = 3 independent assays with SD, analyzed by Ordinary one-way ANOVA.

(B) SUMO1 or SUMO2 knockdowns reduced protein SUMOylation. Lysates of uninfected THP1 macrophages depleted of SUMO1 or SUMO2 were submitted to immunoblot for SUMO1 and SUMO2. Knockdown of SUMO1 specifically reduced SUMO1 conjugate proteins, knockdown of SUMO2 reduced SUMO2 conjugates and high molecular weight SUMO1 conjugated proteins.

(C and D) SUMO1 and SUMO2 knockdown significantly increased parasite proliferation. PMA-induced macrophages were infected with amastigotes and parasite loads in knockdown and control cell lines scored. The number of parasites/100 macrophages was higher at 96 h p.i. in SUMO-depleted cells, including significantly increased parasite loads when normalized relative to 2 h p.i. Mean of three independent samples with SD, each with at least 256 cells, analyzed by two-way ANOVA and Tukey multi-comparison test.

(E and F) Constitute expression of HA-SUMO2 reduced parasite loads in THP-1 macrophages compared to cells transduced with control lentivirus. The relative increase of parasites is also lower in SUMO2 expressing macrophages (F).

**Figure 3. *Continued***

Mean of three independent biological replicates with SD, each replicate with least 120 cells, analyzed by two-way ANOVA and Tukey multi-comparison test.

(G and H) SUMO depletion promoted PVs enlargement. Control and SUMO knockdown THP-1 macrophages were infected with *L. amazonensis* amastigotes for 24 h and PV size measured microscopically. A typical microscopic image is presented in (G). Mean of at least 180 PVs measured for each condition from two independent assays, box and whiskers graph with bars representing 10%-90% range, analyzed by one way ANOVA and Kruskal-Wallis multi-comparison test. Scale bar: 5 μm.

THP-1 macrophages, control and SUMO-depleted, were infected with amastigotes and expression of *ATP6V0D2* and *CD36* determined by qRT-PCR. In wildtype cells, infection significantly increased the expression of *ATP6V0D2* about 3-fold at 6 h which then decreased to less than 2-fold at 24 h pi (Figure 4A). Moreover, SUMO1 and SUMO2 depleted macrophages presented higher levels of *ATP6V0D2* expression before infection, compared to uninfected control cell lines transduced with non-targeting shRNA. After infection, *ATP6V0D2* expression was further induced in the SUMO depleted macrophages, at both 6 and 24 h after infection, compared with control macrophages, and showed enhanced induction compared to the uninfected knockdowns (Figure 4A). The effects on *CD36* expression were less pronounced; it was not changed by amastigote infection in control cells, but SUMO1 knockdown caused a significantly elevation of this lipid receptor at 24 h after infection, when compared to cells transduced with control shRNA, and SUMO2 knockdown promoted higher levels of CD36 before and 24 h after infection (Figure 4B). Importantly, cellular lysates from SUMO depleted cells contained higher levels of total cholesterols measured in cell lysates (Figure 4C). Together, these data suggest ATP6V0D2 and CD36 expression and cholesterol levels are modulated by protein SUMOylation.

It was previously shown that knockdown of *Atp6v0d2* reduces the macrophage overall cholesterol levels and impairs PV biogenesis (Pessoa et al., 2019). To evaluate if *Atp6v0d2* induction is sufficient for the changes in cholesterol levels and PV biogenesis observed in SUMO depleted macrophages we generated RAW 264.7 macrophages stably expressing this gene. Note, THP-1 cells were not used in these experiments because constitutive *ATP6V0D2* expression was toxic to THP-1 cells. Similar to SUMO depleted THP-1 macrophages, *Atp6v0d2* overexpression in RAW 264.7 macrophages strongly promoted PV biogenesis in comparison to control cells transduced with empty plasmid, similar to that observed in SUMO depleted THP-1 macrophages (Figures 5D and 5E). Moreover, *ATP6V0D2* expressing RAW 264.7 cells presented higher levels of free cholesterols compared to control cells transduced with empty vectors (CTRL) (Figure 5A). Using quantitative microscopy and Filipin staining, higher levels of cholesterol were detected in the parasite/PV area (amastigote area plus an additional 5 μm area surrounding each parasite) (Figure 5B). Consistent with the elevated levels of cholesterol in these cells and parasites, constitutive expression of *ATP6V0D2* also induced CD36 expression, a known cholesterol transporter (Figure 5C).

To examine if SUMOylation inhibition modulates cholesterol biosynthesis, as well as import, we determined the gene expression of two key enzymes in cholesterol biosynthesis pathway, *HMGCR* and *SQLE* in SUMO depleted macrophages. Interestingly, *L. mexicana*, which is large PV species in the same group of *L. amazonensis*, is known to upregulate the expression of cholesterol biosynthesis pathway genes to favor macrophage infection (Semini et al., 2017). However, infection with *L. amazonensis* amastigotes did not change the expression of HMGCR and SQLE in wild-type THP-1 macrophages (see Figure S4), but knockdown of SUMO2 slightly enhanced expression *SQLE* in uninfected and infected cells. SUMO1 knockdown enhanced the expression of *HMGCR* and *SQLE* only at 24 h after infection (see Figure S4).

Together, these results show that intracellular amastigotes inhibit SUMOylation to increase cholesterol levels in macrophages through increased expression of *ATP6V0D2, CD36*, and possibly also cholesterol biosynthetic genes. The increased levels of cholesterol correlate with PV enlargement and parasite proliferation, in human and mouse macrophages, and is consistent with earlier publications linking PV biogenesis to macrophage cholesterol retention (Pessoa et al., 2019).

## DISCUSSION

This work began with a genome-wide RNAi screen in *Drosophila* SL2 cells to identify novel factors involved in *L. amazonensis* amastigote infection. The screen was designed to identify factors involved in the initial infection steps, when phagocytes recognize and engulf parasites, potentially triggering cellular responses that can affect the downstream fate of infection such as PV biogenesis. *Drosophila* phagocytes have been successfully used to

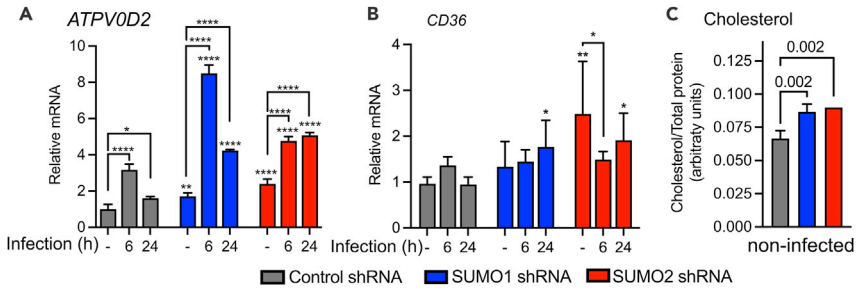


**Figure 4. SUMO depletion increases *ATP6V0D2* and *CD36* expression and elevates cholesterol levels**

THP-1 macrophages were infected and at indicated times, gene expression determined by qRT-PCR whereas free cholesterol was quantified by Cholesterol/Cholesterol ester-Glo Assay in uninfected cells.

(A) *ATP6V0D2* expression is induced by infection and enhanced by SUMO1 or SUMO2 knockdown.

(B) *CD36* expression was not induced by infection but the overall expression was higher in SUMO depleted cells.

(C) Quantitation of free Cholesterol of total lysates shows higher levels in SUMO depleted macrophages. qRT-PCR results from 3 independent biological replicates, analyzed by two-way ANOVA, Sidak's multi-comparison test. The marks on top of each column represent p values compared to the control cells (non-targeting shRNA transduced, gray bars), whereas the bracketed marks indicated comparison within knockdown groups. Error bars represent one SD. *, $p \leq 0.05$; **, $p \leq 0.01$; ***, $p \leq 0.001$; ****, $p \leq 0.0001$. Cholesterol quantification (C) was analyzed by one-way ANOVA, 3 biological replicates.

study several human pathogens, including intracellular bacteria, viruses, and protozoan parasites (Agaisse et al., 2005; Cheng and Portnoy, 2003; Cherry et al., 2005, 2006; Peltan et al., 2012; Philips et al., 2005). The conservation of key recognition and signaling pathways involved in host defense and phagocytosis, including *Leishmania* uptake, was highlighted by the findings from our screen where 52 of 55 genes identified for their specific effects on *L. amazonensis* infection, are conserved between insects and humans.

We did not find common hits between our results and the published work from Peltan et al. (2012), who screened for *Leishmania donovani* amastigote infection factors also in *Drosophila* S2 cells (Peltan et al., 2012). This result could be expected because the large phylogenetic distance between these two New World *Leishmania* species. Another explanation for the lack of concordance is that *L. donovani* screen examined only a small fraction of the genome, a dsRNA library with only 1,920 genes, compared to our genome-wide library targeting 13,071 genes. The library used for *L. donovani* screen did not contain, for example, three SUMOylation factors, AOS1, Su(var)2–10 and UBA2, identified in our screen. Also, Peltan et al. (2012) did determine if the genes identified in their screen specifically affected in *Leishmania* parasite - host interactions, as opposed to identifying genes non-specifically involved in phagocytosis.

Based on the strong SUMOylation signature in the screen results, we explored the role of SUMOylation in *Leishmania* infection of mammalian macrophages. Of interest, amastigote, but not promastigote, infection quickly and potently inhibited host SUMOylation in both human and mouse macrophages, even inhibiting the induction of SUMO conjugation observed with heat shock. This drastic protein deSUMOylation seems to favor infection because knockdown of SUMOylation factors prior to infection caused higher proliferation of amastigotes within larger macrophages PVs. Together these data suggest *L. amazonensis* amastigotes actively interfere with the host cell SUMO machinery to enhance their own replicative niche.

Intriguingly, knockdown of SUMOylation factors provoked different outcomes in the infection of *Drosophila* and mammalian macrophages. The uptake of parasites was reduced by knockdown of SUMO factors in SL2 cell assays, but not in mammalian macrophages. On the other hand, knockdown of SUMO factors favored intracellular proliferation of amastigotes within macrophages, a phenotype that we could not assess in SL2 cells because *L. amazonensis* did not grow within these cells. One possible explanation for the unsuccessful parasite growth in SL2 cells is the temperature incompatibility, in natural infection of mammalian skin, parasites grow at a temperature of approximately 34 °C and SL2 are cultured at 27°C. Because of this technical limitation of Drosophila model, after the identification of hits we focused our studies on the infection of mammalian macrophages and the role of candidates from our screen in these models, which are most relevant to human infections.

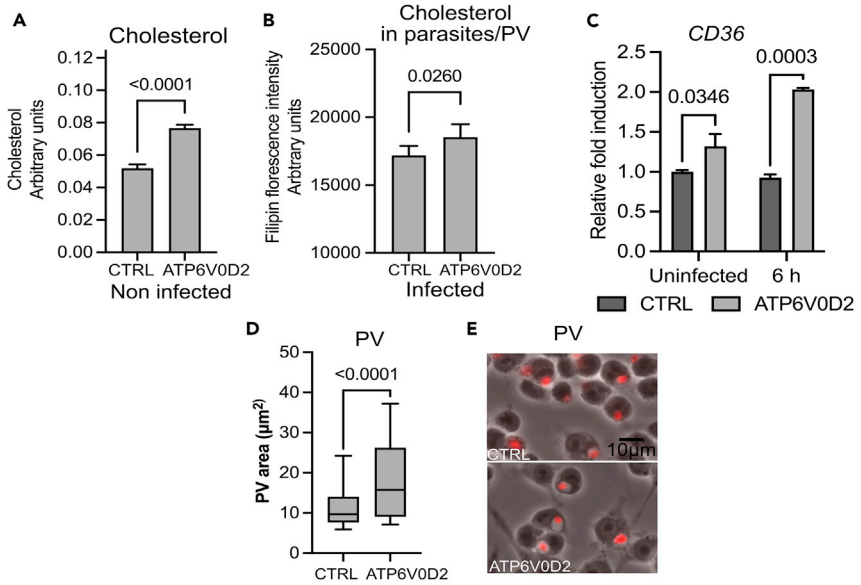


**Figure 5. *Atp6v0d2* expression increases free cholesterol levels and favors PV enlargement and in RAW 264.7 macrophages**

RAW 264.7 macrophages were transduced with a control lentivirus (CTRL) or with a lentivirus to promote constitutive expression of *Atp6v0d2*.

(A) *Atp6v0d2* expressing cells show increased cholesterol levels in total lysates compared to control.

(B) Macrophages were infected with amastigotes for 6 h, fixed and cholesterol stained with filipin. The filipin fluorescence intensity was quantified in parasite area and 5 µm surrounding to include the PV. Macrophages expressing *ATP6V0D2* presented higher cholesterol levels compared to the control. Constitutive expression of ATP6V0D2 also induced higher *CD36* expression (C) and larger amastigote-containing PV (D and E) compared to controls at 6 h after infection. Statistical analysis: A-B, representative results of 3 independent experiments each with at least 4 independent replicates, Error bars represent one SD, analyzed by t-test; C, representative data of 3 independent experiments each with at least 3 independent replicates with SD, two-way ANOVA with Sidak's multi-comparison test; D, at least 120 PV per sample, plotted in a box and whiskers graph, wiskers represent 10%-90% range. The data were analysed using t-test. (E) Representative images from at least 3 indpendent data sets.

SUMO regulates numerous cellular functions and activities, and human cells have 3,500 to 6,700 SUMOylated proteins, many of them SUMOylated on multiple residues (Hendriks et al., 2017; Lamoliatte et al., 2017; Mattoscio et al., 2013; Wimmer and Schreiner, 2015). Not surprisingly, many pathogens sabotage this post-translational modification to facilitate infection. For example, bacteria *Salmonella typhimurium*, *Listeria monocytogenes*, *Shigella flexneri*, and *Yersinia pestis* actively interfere in the SUMOylation machinery during intracellular invasion (Fritah et al., 2014; Orth et al., 2000; Ribet et al., 2010; Sidik et al., 2015). DeSUMOylation caused by *L. monocytogenes* inhibits TGF beta signaling, whereas *S. flexneri*-induced deSUMOylation increases permeability of the gut, favoring bacterial invasion and induces an exacerbated inflammatory response in mice (Fritah et al., 2014). Intracellular *S. typhimurium* reduces Rab7 SUMOylation and favors the formation of *Salmonella*-induced membrane filaments radiating from the Salmonella-containing vacuole which improves bacteria survival (Mohapatra et al., 2019). Finally, two protozoan parasites, which also live in PVs, *Plasmodium berghei* and *Toxoplasma gondii*, reduce protein SUMOylation to inhibit nuclear translocation of immune induced transcription factors, such as SMAD4, thereby reducing cellular responses to infection, resisting apoptosis, and favoring parasite infection (Maruthi et al., 2017).

Our data support the hypothesis that amastigotes cause a rapid inhibition of host protein SUMOylation to induce *ATP6V0D2* expression, increase cholesterol levels, and support PV enlargement to facilitate survival of intracellular amastigotes. The enlarged PV, typical of parasites from the *L. mexicana* group, is a specialized organelle that protects the intracellular parasites from anti-parasitic host defense such as nitric oxide (Wilson et al., 2008). PV enlargement is actively driven by amastigotes, which manipulate macrophage vesicle trafficking and lipid metabolism/transport for this purpose (Courret et al., 2002; Young and Kima, 2019). Using *Atp6v0d2* loss of function approaches, Pessoa et al. (2019) showed that Atp6v0d2 controls

PV enlargement, *Cd36* expression and cholesterol levels in macrophages. Our studies complement and extend those earlier studies by revealing key role for parasite-triggered deSUMOylation in controlling *ATP6V0D2*, *CD36*, *HMGCR* and *SQLE* expression and cholesterol levels.

Atp6v0d subunits are best known as a component of vacuolar-ATPases. V-ATPases are multiunit complexes composed of two domains: $V_1$ domain, responsible for ATP hydrolysis and generation of energy for the proton translocation through the integral $V_0$ domain. Atp6v0d subunits are part of the $V_0$ domain and form a connective stalk between subunits $V_0$ and V1. Although V-ATPases are present in all cells, the *Atp6v0d2* isoform is expressed in specific tissues (renal, epididymis, osteoclast, dendritic cells, macrophages), whereas the more common d-subunit, Atp6v0d1 is expressed ubiquitously (Liu et al., 2019; Toei et al., 2010). More recently, Atp6v0d2 has been shown to participate in several cellular processes distinct from V-ATPase activity, including the degradation of transcription factors (Liu et al., 2019), inflammasome activation (Xia et al., 2019), the fusion of osteoblasts (Kim et al., 2008), and autophagosome-lysosome fusion. These last two findings suggests that this alternate V-ATPase subunit function could be involved in PV biogenenesis by controlling vesicular membrane fusion. One interesting hypothesis is that ATP6V0D2 interacts with VAMP8 to promote fusion of endocytic organelles to *Leishmania* PVs, as interaction of ATP6V0D2 with VAMP8 has been shown to control autophagosome-lysosome fusion during *S. typhimurium* infection (Furuta et al., 2010) whereas VAMP8 is also linked to fusion of endocytic vesicles the *L. amazonensis* PV (Seguin et al., 2022).

One unanswered question is how SUMOylation inhibition promotes *ATP6V0D2* expression. The role of SUMOylation in the control of gene expression is well-established, particularly via the SUMOylation of transcription factors (Boulanger et al., 2021). Although the effect of transcription factor SUMOylation varies, in most cases it reduces transcription of target genes (Rosonina et al., 2017). Of interest, a publicly available ChIP-seq dataset from mouse dendritic cells shows that a 588 bp DNA region, 32kb upstream of *Atp6v0d2*, is significantly enriched in SUMO2-conjugated chromatin (Decque et al., 2016). Therefore, one possibility is that amastigote-induced deSUMOylation of transcription factor(s), which bind this element near *Atp6v0d2*, drive higher expression of *Atp6v0d2*. Some potential candidates are the transcription factors CTCF, RAD21, Zinc finger protein 143, c-FOS and PPARγ, whose activities are known to be modulated by SUMOylation and are linked in *Atp6v0d2* expression (Jennewein et al., 2008; Stelzer et al., 2016).

In summary, our *Drosophila* screen effectively identified novel host factors involved in *Leishmania*-host cell interactions. Our results implicate a novel *L. amazonensis* virulence strategy, whereby amastigotes drastically reduce host cell protein SUMOylation to drive increased *ATP6V0D2*, CD36, *HMGCR* and *SQLE* expression and consequently higher cholesterol availability, as a strategy to promote their own proliferation. The *Leishmania* PV has clear parallels to the replicative niche of other intracellular bacterial pathogens and it will be interesting to learn from future studies if similar processes are involved. Further in-depth studies focused on the mechanistic interactions between protein SUMOylation and parasite growth, as well as on the other hits found in the *Drosophila* screen may reveal new targets for leishmaniasis treatment.

## Limitations of the study

Perhaps the most important limitation of this study is the lack of an *in vivo* infection study. These studies are essential to validate our *in vitro* findings in the complex skin infection environment. Another important question this work did not address is if SUMOylation inhibition is a virulence mechanism specific for *L. amazonensis*, for other large PV *Leishmania* species, or is similar in all pathogenic *Leishmania*. Finally, using *Drosophila* systems has a screening platform has inherent caveats as parasite-host interactions may differ between insects and mammals, and any potential candidates from these screens require thorough investigation and validation in mammalian system as performed here for SUMO.

## STAR★METHODS

Detailed methods are provided in the online version of this paper and include the following:

- KEY RESOURCES TABLE
- RESOURCE AVAILABILITY
  - Lead contact
  - Materials availability
  - Data and code availability

- EXPERIMENTAL MODEL AND SUBJECT DETAILS
  - Ethics statement: Our lab conducted all experiments according to the guidelines of the American Association for Laboratory Animal Science and approved by the Institutional Animal Care and Use Committee at the University of Massachusetts Medical School (Docket#: A-2056-19).Drosophila SL2 cells
  - Mouse bone marrow derive macrophages (BMDM)
  - Leishmania amazonensis
  - THP-1
  - RAW 264.7
- METHOD DETAILS
  - Confocal microscopy
  - HTS screening
  - dsRNA synthesis and secondary screen
  - Phagocytosis of *E. coli* and *S. aureus*
  - Bioinformatic analysis
  - Macrophage transduction
  - Western blot
  - Production of retroviral vectors and transduction of immortalized mouse macrophages
  - ATP6V0D2 plasmid
  - Macrophage infection and PV area measurement
  - Cholesterol localization using filipin staining
  - RNA and qRT–PCR
  - Cholesterol measurement
- QUANTIFICATION AND STATISTICAL ANALYSIS

## SUPPLEMENTAL INFORMATION

Supplemental information can be found online at https://doi.org/10.1016/j.isci.2022.104909.

## ACKNOWLEDGMENTS

This work was supported by NIH/NIAID United States: R21AI154208 and R21AI136532. We thank Javier Irazoqui and Havisha Honwad for the help on TFEB studies, Jeremy Kay for helping in the studies on DRAPER mouse orthologs, Jie Xu for assistance on HTS.

## AUTHOR CONTRIBUTIONS

Conceptualization, K.O., M.R., S.C., and N.S., Methodology, N.S, S.C., K.O., M.R., and R.G., Formal Analysis, K.O., Investigation, K.O., M.M.S.C.F., and A.Y., Resources, N.S. and S.C., Writing – Original Draft, N.S. and K.O., Writing – Review and Editing, N.S. and K.O., Visualization, N.S. and K.O., Supervision, N.S., Project Administration, N.S., S.C. and K.O., Funding Acquisition, N.S. and K.O.

## DECLARATION OF INTERESTS

The authors declare no competing interests.

Received: May 9, 2022
Revised: June 29, 2022
Accepted: August 5, 2022
Published: September 16, 2022

## REFERENCES

Agaisse, H., Burrack, L.S., Philips, J.A., Rubin, E.J., Perrimon, N., and Higgins, D.E. (2005). Genome-wide RNAi screen for host factors required for intracellular bacterial infection. Science *309*, 1248–1251. https://doi.org/10.1126/science.1116008.

Alvar, J., Vélez, I.D., Bern, C., Herrero, M., Desjeux, P., Cano, J., Jannin, J., and den Boer, M.; WHO Leishmaniasis Control Team (2012). Leishmaniasis worldwide and global estimates of its incidence. PLoS One *7*, e35671. https://doi.org/10.1371/journal.pone.0035671.

Bekes, M., Prudden, J., Srikumar, T., Raught, B., Boddy, M.N., and Salvesen, G.S. (2011). The dynamics and mechanism of SUMO chain deconjugation by SUMO-specific proteases. J. Biol. Chem. *286*, 10238–10247. https://doi.org/10.1074/jbc.M110.205153.

Boulanger, M., Chakraborty, M., Tempé, D., Piechaczyk, M., and Bossis, G. (2021). SUMO and transcriptional regulation: the lessons of large-scale proteomic. Molecules *26*, 828. https://doi.org/10.3390/molecules26040828.

Cameron, P., McGachy, A., Anderson, M., Paul, A., Coombs, G.H., Mottram, J.C., Alexander, J., and Plevin, R. (2004). Inhibition of lipopolysaccharide-induced macrophage IL-12

production by Leishmania mexicana amastigotes: the role of cysteine peptidases and the NF-kappaB signaling pathway. J. Immunol. *173*, 3297–3304.

Cheng, L.W., and Portnoy, D.A. (2003). Drosophila S2 cells: an alternative infection model for Listeria monocytogenes. Cell Microbiol. *5*, 875–885.

Cherry, S., Doukas, T., Armknecht, S., Whelan, S., Wang, H., Sarnow, P., and Perrimon, N. (2005). Genome-wide RNAi screen reveals a specific sensitivity of IRES-containing RNA viruses to host translation inhibition. Genes Dev. *19*, 445–452. https://doi.org/10.1101/gad.1267905.

Cherry, S., Kunte, A., Wang, H., Coyne, C., Rawson, R.B., and Perrimon, N. (2006). COPI activity coupled with fatty acid biosynthesis is required for viral replication. PLoS Pathog. *2*, e102. https://doi.org/10.1371/journal.ppat.0020102.

Contreras, I., Gómez, M.A., Nguyen, O., Shio, M.T., McMaster, R.W., and Olivier, M. (2010). Leishmania-induced inactivation of the macrophage transcription factor AP-1 is mediated by the parasite metalloprotease GP63. PLoS Pathog. *6*, e1001148. https://doi.org/10.1371/journal.ppat.1001148.

Courret, N., Fréhel, C., Gouhier, N., Pouchelet, M., Prina, E., Roux, P., and Antoine, J.C. (2002). Biogenesis of Leishmania-harbouring parasitophorous vacuoles following phagocytosis of the metacyclic promastigote or amastigote stages of the parasites. J. Cell Sci. *115*, 2303–2316.

Courret, N., Frehel, C., Prina, E., Lang, T., and Antoine, J.C. (2001). Kinetics of the intracellular differentiation of Leishmania amazonensis and internalization of host MHC molecules by the intermediate parasite stages. Parasitology *122*, 263–279.

de Araujo Soares, R.M., dos Santos, A.L., Bonaldo, M.C., de Andrade, A.F., Alviano, C.S., Angluster, J., and Goldenberg, S. (2003). Leishmania (Leishmania) amazonensis: differential expression of proteinases and cell-surface polypeptides in avirulent and virulent promastigotes. Exp. Parasitol. *104*, 104–112.

Decque, A., Joffre, O., Magalhaes, J.G., Cossec, J.C., Blecher-Gonen, R., Lapaquette, P., Silvin, A., Manel, N., Joubert, P.E., Seeler, J.S., et al. (2016). Sumoylation coordinates the repression of inflammatory and anti-viral gene-expression programs during innate sensing. Nat. Immunol. *17*, 140–149. https://doi.org/10.1038/ni.3342.

Dutta, S., Ray, D., Kolli, B.K., and Chang, K.P. (2005). Photodynamic sensitization of Leishmania amazonensis in both extracellular and intracellular stages with aluminum phthalocyanine chloride for photolysis in vitro. Antimicrob. Agents Chemother. *49*, 4474–4484. https://doi.org/10.1128/AAC.49.11.4474-4484.2005.

Flotho, A., and Melchior, F. (2013). Sumoylation: a regulatory protein modification in health and disease. Annu. Rev. Biochem. *82*, 357–385. https://doi.org/10.1146/annurev-biochem-061909-093311.

Fritah, S., Lhocine, N., Golebiowski, F., Mounier, J., Andrieux, A., Jouvion, G., Hay, R.T., Sansonetti, P., and Dejean, A. (2014). Sumoylation controls host anti-bacterial response to the gut invasive pathogen Shigella flexneri. EMBO Rep. *15*, 965–972. https://doi.org/10.15252/embr.201338386.

Furuta, N., Fujita, N., Noda, T., Yoshimori, T., and Amano, A. (2010). Combinational soluble N-ethylmaleimide-sensitive factor attachment protein receptor proteins VAMP8 and Vti1b mediate fusion of antimicrobial and canonical autophagosomes with lysosomes. Mol. Biol. Cell *21*, 1001–1010. https://doi.org/10.1091/mbc.E09-08-0693.

Gill, G. (2004). SUMO and ubiquitin in the nucleus: different functions, similar mechanisms? Genes Dev. *18*, 2046–2059. https://doi.org/10.1101/gad.1214604.

Gold, K.S., and Bruckner, K. (2015). Macrophages and cellular immunity in Drosophila melanogaster. Semin. Immunol. *27*, 357–368. https://doi.org/10.1016/j.smim.2016.03.010.

Guy, R.A., and Belosevic, M. (1993). Comparison of receptors required for entry of Leishmania major amastigotes into macrophages. Infect. Immun. *61*, 1553–1558.

Hackam, D.J., Botelho, R.J., Sjolin, C., Rotstein, O.D., Robinson, J.M., Schreiber, A.D., and Grinstein, S. (2001). Indirect role for COPI in the completion of FCgamma receptor-mediated phagocytosis. J. Biol. Chem. *276*, 18200–18208. https://doi.org/10.1074/jbc.M102009200.

Halle, M., Gomez, M.A., Stuible, M., Shimizu, H., McMaster, W.R., Olivier, M., and Tremblay, M.L. (2009). The Leishmania surface protease GP63 cleaves multiple intracellular proteins and actively participates in p38 mitogen-activated protein kinase inactivation. J. Biol. Chem. *284*, 6893–6908. https://doi.org/10.1074/jbc.M805861200.

Hendriks, I.A., Lyon, D., Young, C., Jensen, L.J., Vertegaal, A.C.O., and Nielsen, M.L. (2017). Site-specific mapping of the human SUMO proteome reveals co-modification with phosphorylation. Nat. Struct. Mol. Biol. *24*, 325–336. https://doi.org/10.1038/nsmb.3366.

Hu, Y., Comjean, A., Roesel, C., Vinayagam, A., Flockhart, I., Zirin, J., Perkins, L., Perrimon, N., and Mohr, S.E. (2017). FlyRNAi.org-the database of the Drosophila RNAi screening center and transgenic RNAi project: 2017 update. Nucleic Acids Res. *45*, D672–D678. https://doi.org/10.1093/nar/gkw977.

Isnard, A., Shio, M.T., and Olivier, M. (2012). Impact of Leishmania metalloprotease GP63 on macrophage signaling. Front. Cell. Infect. Microbiol. *2*, 72. https://doi.org/10.3389/fcimb.2012.00072.

Jennewein, C., Kuhn, A.M., Schmidt, M.V., Meilladec-Jullig, V., von Knethen, A., Gonzalez, F.J., and Brüne, B. (2008). Sumoylation of peroxisome proliferator-activated receptor gamma by apoptotic cells prevents lipopolysaccharide-induced NCoR removal from kappaB binding sites mediating transrepression of proinflammatory cytokines. J. Immunol. *181*, 5646–5652. https://doi.org/10.4049/jimmunol.181.8.5646.

Kim, K., Lee, S.H., Ha Kim, J., Choi, Y., and Kim, N. (2008). NFATc1 induces osteoclast fusion via up-regulation of Atp6v0d2 and the dendritic cell-specific transmembrane protein (DC-STAMP). Mol. Endocrinol. *22*, 176–185. https://doi.org/10.1210/me.2007-0237.

Kima, P.E. (2014). Leishmania molecules that mediate intracellular pathogenesis. Microbes Infect. *16*, 721–726. https://doi.org/10.1016/j.micinf.2014.07.012.

Lamoliatte, F., McManus, F.P., Maarifi, G., Chelbi-Alix, M.K., and Thibault, P. (2017). Uncovering the SUMOylation and ubiquitylation crosstalk in human cells using sequential peptide immunopurification. Nat. Commun. *8*, 14109. https://doi.org/10.1038/ncomms14109.

Liu, N., Luo, J., Kuang, D., Xu, S., Duan, Y., Xia, Y., Wei, Z., Xie, X., Yin, B., Chen, F., et al. (2019). Lactate inhibits ATP6V0d2 expression in tumor-associated macrophages to promote HIF-2alpha-mediated tumor progression. J. Clin. Invest. *129*, 631–646. https://doi.org/10.1172/JCI123027.

Love, D.C., Mentink Kane, M., and Mosser, D.M. (1998). Leishmania amazonensis: the phagocytosis of amastigotes by macrophages. Exp. Parasitol. *88*, 161–171.

Lowrey, A.J., Cramblet, W., and Bentz, G.L. (2017). Viral manipulation of the cellular sumoylation machinery. Cell Commun. Signal. *15*, 27. https://doi.org/10.1186/s12964-017-0183-0.

Maruthi, M., Singh, D., Reddy, S.R., Mastan, B.S., Mishra, S., and Kumar, K.A. (2017). Modulation of host cell SUMOylation facilitates efficient development of Plasmodium berghei and Toxoplasma gondii. Cell Microbiol. *19*, e12723. https://doi.org/10.1111/cmi.12723.

Mattoscio, D., Segré, C.V., and Chiocca, S. (2013). Viral manipulation of cellular protein conjugation pathways: the SUMO lesson. World J. Virol. *2*, 79–90. https://doi.org/10.5501/wjv.v2.i2.79.

Mehta, S.R., Zhang, X.Q., Badaro, R., Spina, C., Day, J., Chang, K.P., and Schooley, R.T. (2010). Flow cytometric screening for anti-leishmanials in a human macrophage cell line. Exp. Parasitol. *126*, 617–620. https://doi.org/10.1016/j.exppara.2010.06.007.

Mi, H., Muruganujan, A., Ebert, D., Huang, X., and Thomas, P.D. (2019). PANTHER version 14: more genomes, a new PANTHER GO-slim and improvements in enrichment analysis tools. Nucleic Acids Res. *47*, D419–D426. https://doi.org/10.1093/nar/gky1038.

Mohapatra, G., Gaur, P., Mujagond, P., Singh, M., Rana, S., Pratap, S., Kaur, N., Verma, S., Krishnan, V., Singh, N., and Srikanth, C.V. (2019). A SUMOylation-dependent switch of RAB7 governs intracellular life and pathogenesis of Salmonella Typhimurium. J. Cell Sci. *132*, jcs222612. https://doi.org/10.1242/jcs.222612.

Morehead, J., Coppens, I., and Andrews, N.W. (2002). Opsonization modulates Rac-1 activation during cell entry by Leishmania amazonensis. Infect. Immun. *70*, 4571–4580. https://doi.org/10.1128/iai.70.8.4571-4580.2002.

Mottram, J.C., Coombs, G.H., and Alexander, J. (2004). Cysteine peptidases as virulence factors of Leishmania. Curr. Opin. Microbiol. *7*, 375–381. https://doi.org/10.1016/j.mib.2004.06.010.

Niskanen, E.A., Malinen, M., Sutinen, P., Toropainen, S., Paakinaho, V., Vihervaara, A., Joutsen, J., Kaikkonen, M.U., Sistonen, L., and Palvimo, J.J. (2015). Global SUMOylation on active chromatin is an acute heat stress response restricting transcription. Genome Biol. *16*, 153. https://doi.org/10.1186/s13059-015-0717-y.

Okuda, K., Tong, M., Dempsey, B., Moore, K.J., Gazzinelli, R.T., and Silverman, N. (2016). Leishmania amazonensis engages CD36 to drive parasitophorous vacuole maturation. PLoS Pathog. *12*, e1005669. https://doi.org/10.1371/journal.ppat.1005669.

Olivier, M., Gregory, D.J., and Forget, G. (2005). Subversion mechanisms by which Leishmania parasites can escape the host immune response: a signaling point of view. Clin. Microbiol. Rev. *18*, 293–305. https://doi.org/10.1128/CMR.18.2.293-305.2005.

Orth, K., Xu, Z., Mudgett, M.B., Bao, Z.Q., Palmer, L.E., Bliska, J.B., Mangel, W.F., Staskawicz, B., and Dixon, J.E. (2000). Disruption of signaling by Yersinia effector YopJ, a ubiquitin-like protein protease. Science *290*, 1594–1597. https://doi.org/10.1126/science.290.5496.1594.

Peltan, A., Briggs, L., Matthews, G., Sweeney, S.T., and Smith, D.F. (2012). Identification of Drosophila gene products required for phagocytosis of Leishmania donovani. PLoS One *7*, e51831. https://doi.org/10.1371/journal.pone.0051831.

Pessoa, C.C., Reis, L.C., Ramos-Sanchez, E.M., Orikaza, C.M., Cortez, C., de Castro Levatti, E.V., Badaró, A.C.B., Yamamoto, J.U.d.S., D'Almeida, V., Goto, H., et al. (2019). ATP6V0d2 controls Leishmania parasitophorous vacuole biogenesis via cholesterol homeostasis. PLoS Pathog. *15*, e1007834. https://doi.org/10.1371/journal.ppat.1007834.

Peters, C., Aebischer, T., Stierhof, Y.D., Fuchs, M., and Overath, P. (1995). The role of macrophage receptors in adhesion and uptake of leishmania-mexicana amastigotes. J. Cell Sci. *108*, 3715–3724.

Philips, J.A., Rubin, E.J., and Perrimon, N. (2005). Drosophila RNAi screen reveals CD36 family member required for mycobacterial infection. Science *309*, 1251–1253. https://doi.org/10.1126/science.1116006.

Ramet, M., Manfruelli, P., Pearson, A., Mathey-Prevot, B., and Ezekowitz, R.A.B. (2002). Functional genomic analysis of phagocytosis and identification of a Drosophila receptor for E. coli. Nature *416*, 644–648. https://doi.org/10.1038/nature735.

Ribet, D., and Cossart, P. (2018). Ubiquitin, SUMO, and NEDD8: key targets of bacterial pathogens. Trends Cell Biol. *28*, 926–940. https://doi.org/10.1016/j.tcb.2018.07.005.

Ribet, D., Hamon, M., Gouin, E., Nahori, M.A., Impens, F., Neyret-Kahn, H., Gevaert, K., Vandekerckhove, J., Dejean, A., and Cossart, P. (2010). Listeria monocytogenes impairs SUMOylation for efficient infection. Nature *464*, 1192–1195. https://doi.org/10.1038/nature08963.

Rosonina, E., Akhter, A., Dou, Y., Babu, J., and Sri Theivakadadcham, V.S. (2017). Regulation of transcription factors by sumoylation. Transcription *8*, 220–231. https://doi.org/10.1080/21541264.2017.1311829.

Schindelin, J., Arganda-Carreras, I., Frise, E., Kaynig, V., Longair, M., Pietzsch, T., Preibisch, S., Rueden, C., Saalfeld, S., Schmid, B., et al. (2012). Fiji: an open-source platform for biological-image analysis. Nat. Methods *9*, 676–682. https://doi.org/10.1038/nmeth.2019.

Schneider, I. (1972). Cell lines derived from late embryonic stages of Drosophila melanogaster. J. Embryol. Exp. Morphol. *27*, 353–365.

Seguin, O., Mai, L.T., Acevedo Ospina, H., Guay-Vincent, M.M., Whiteheart, S.W., Stäger, S., and Descoteaux, A. (2022). VAMP3 and VAMP8 regulate the development and functionality of parasitophorous vacuoles housing Leishmania amazonensis. Infect. Immun. *90*, e0018321. https://doi.org/10.1128/IAI.00183-21.

Seifert, A., Schofield, P., Barton, G.J., and Hay, R.T. (2015). Proteotoxic stress reprograms the chromatin landscape of SUMO modification. Sci. Signal. *8*, rs7. https://doi.org/10.1126/scisignal.aaa2213.

Semini, G., Paape, D., Paterou, A., Schroeder, J., Barrios-Llerena, M., and Aebischer, T. (2017). Changes to cholesterol trafficking in macrophages by Leishmania parasites infection. Microbiologyopen *6*, e00469. https://doi.org/10.1002/mbo3.469.

Sidik, S.M., Salsman, J., Dellaire, G., and Rohde, J.R. (2015). Shigella infection interferes with SUMOylation and increases PML-NB number. PLoS One *10*, e0122585. https://doi.org/10.1371/journal.pone.0122585.

Stelzer, G., Rosen, N., Plaschkes, I., Zimmerman, S., Twik, M., Fishilevich, S., Stein, T.I., Nudel, R., Lieder, I., Mazor, Y., et al. (2016). The GeneCards suite: from gene data mining to disease genome sequence analyses. Curr. Protoc. Bioinform. *54*, 1.30.1–1.30.33. https://doi.org/10.1002/cpbi.5.

Thomas, P.D., Campbell, M.J., Kejariwal, A., Mi, H., Karlak, B., Daverman, R., Diemer, K., Muruganujan, A., and Narechania, A. (2003). PANTHER: a library of protein families and subfamilies indexed by function. Genome Res. *13*, 2129–2141. https://doi.org/10.1101/gr.772403.

Toei, M., Saum, R., and Forgac, M. (2010). Regulation and isoform function of the V-ATPases. Biochemistry *49*, 4715–4723. https://doi.org/10.1021/bi100397s.

Ueno, N., and Wilson, M.E. (2012). Receptor-mediated phagocytosis of Leishmania: implications for intracellular survival. Trends Parasitol. *28*, 335–344. https://doi.org/10.1016/j.pt.2012.05.002.

Verma, S., Mohapatra, G., Ahmad, S.M., Rana, S., Jain, S., Khalsa, J.K., and Srikanth, C.V. (2015). Salmonella engages host MicroRNAs to modulate SUMOylation: a new arsenal for intracellular survival. Mol. Cell Biol. *35*, 2932–2946. https://doi.org/10.1128/MCB.00397-15.

Wan, C.P., Park, C.S., and Lau, B.H. (1993). A rapid and simple microfluorometric phagocytosis assay. J. Immunol. Methods *162*, 1–7. https://doi.org/10.1016/0022-1759(93)90400-2.

Wanderley, J.L.M., Pinto da Silva, L.H., Deolindo, P., Soong, L., Borges, V.M., Prates, D.B., de Souza, A.P.A., Barral, A., Balanco, J.M.d.F., do Nascimento, M.T.C., et al. (2009). Cooperation between apoptotic and viable metacyclics enhances the pathogenesis of Leishmaniasis. PLoS One *4*, e5733. https://doi.org/10.1371/journal.pone.0005733.

Wanderley, J.L.M., Thorpe, P.E., Barcinski, M.A., and Soong, L. (2012). Phosphatidylserine exposure on the surface of Leishmania amazonensis amastigotes modulates in vivo infection and dendritic cell function. Parasite Immunol. *35*, 109–119. https://doi.org/10.1111/pim.12019.

Wilson, J., Huynh, C., Kennedy, K.A., Ward, D.M., Kaplan, J., Aderem, A., and Andrews, N.W. (2008). Control of parasitophorous vacuole expansion by LYST/Beige restricts the intracellular growth of Leishmania amazonensis. PLoS Pathog. *4*, e1000179. https://doi.org/10.1371/journal.ppat.1000179.

Wilson, V.G. (2017). Viral interplay with the host sumoylation system. Adv. Exp. Med. Biol. *963*, 359–388. https://doi.org/10.1007/978-3-319-50044-7_21.

Wimmer, P., and Schreiner, S. (2015). Viral mimicry to usurp ubiquitin and SUMO host pathways. Viruses *7*, 4854–4872. https://doi.org/10.3390/v7092849.

Xia, Y., Liu, N., Xie, X., Bi, G., Ba, H., Li, L., Zhang, J., Deng, X., Yao, Y., Tang, Z., et al. (2019). The macrophage-specific V-ATPase subunit ATP6V0D2 restricts inflammasome activation and bacterial infection by facilitating autophagosome-lysosome fusion. Autophagy *15*, 960–975. https://doi.org/10.1080/15548627.2019.1569916.

Young, J., and Kima, P.E. (2019). The Leishmania parasitophorous vacuole membrane at the parasite-host interface. Yale J. Biol. Med. *92*, 511–521.

Zhang, X.D., Yang, X.C., Chung, N., Gates, A., Stec, E., Kunapuli, P., Holder, D.J., Ferrer, M., and Espeseth, A.S. (2006). Robust statistical methods for hit selection in RNA interference high-throughput screening experiments. Pharmacogenomics *7*, 299–309. https://doi.org/10.2217/14622416.7.3.299.

## STAR★METHODS

### KEY RESOURCES TABLE

| REAGENT or RESOURCE | SOURCE | IDENTIFIER |
|---|---|---|
| Antibodies | | |
| Goat anti-mouse AlexaFluor 594 | Invitrogen | A-21205; RRID:AB_2535791 |
| Rabbit anti-SUMO1 | Cell Signalling Technologies | C9H1; RRID:AB_2302825 |
| Rabbit anti-SUMO2/3 | Cell Signalling Techonologies | 18H8; RRID:AB_2198425 |
| Rabbit anti-SAE1 | Invitrogen | PA5-22297; RRID:AB_11153590 |
| Mouse anti-Ubc9 | BD Biosciences | 610748; RRID:AB_398071 |
| Mouse anti-actin,monoclonal (Clone: C4) | MP Biomedicals | 0869100; RRID:AB_2920628 |
| Goat Anti-Rabbit IgG (H+L)-HRP Conjugate | Bio-Rad | 1721019; RRID:AB_11125143 |
| Goat Anti-Mouse IgG (H + L)-HRP Conjugate | BioRad | 1706516; RRID:AB_2921252 |
| Chemicals, peptides, and recombinant proteins | | |
| Sodium succinate dibasic hexahydrate | Sigma Aldrich | S9637 |
| Critical commercial assays | | |
| Lysotracker Blue DND-22 | Invitrogen | L7525 |
| CellMask Deep Red Plasma membrane Stain | Invitrogen | C10046 |
| Silencer Drosophila RNAi Library | Ambion | AM85000 |
| MEGAscript T7 transcription | Invitrogen | AM1334 |
| *Escherichia coli* (K-12 strain) BioParticles™, fluorescein conjugate | Invitrogen | E2861 |
| *Staphylococcus aureus* (Wood strain without protein A) BioParticles™, Alexa Fluor™ 488 conjugate | Invitrogen | S23371 |
| Protein Assay dye | Bio-Rad | 5000006 |
| Trizol | Invitrogen | 15596026 |
| iScript gDNA Clear cDNA synthesis kit | Bio-Rad | 1725035 |
| Cholesterol/Cholesterol Ester-Glo Assay | Promega | J3190 |
| iTaq Universal SYBR Green Supermix | Bio-Rad | 1725121 |
| Clarity™ Western ECL Substrate | BioRad | 1705060 |
| Experimental models: Cell lines | | |
| RAW 264.7 | ATCC | TIB-71; RRID:CVCL_0493 |
| THP-1 | ATCC | TIB-202; RRID:CVCL_0006 |
| SL2 | Schneider, 1972 | N/A |
| Leishmania amazonensis MHOM/BR/ 1973/M2269, GFP expressing | Silvia Reni Bortolin Uliana, University of São Paulo, Brazil | N/A |
| Leishmania amazonensis RAT/BA/LV78, dsRed expressing | Kwang-Poo Chang, Rosalind Franklin University of Medicine and Science | N/A |
| Experimental models: Organisms/strains | | |
| BALB/cJ mouse | The Jackson Laboratories | 000651; RRID:IMSR_JAX:000651 |
| C57BL/6j | The Jackson Laboratories | 000664; RRID:IMSR_JAX:000651 |
| Recombinant DNA | | |
| SUMO1 shRNA, human | Dharmacon | V3LHS_404077 |
| SUMO2 shRNA, human | Dharmacon | V3LHS_412780 |

(*Continued on next page*)

*Continued*

| REAGENT or RESOURCE | SOURCE | IDENTIFIER |
|---|---|---|
| pCMV3-ATP6V0D2-FLAG | Sino Biological | HG23801-CF |
| pcDNA3 HA-SUMO2 | Addgene, PubMed 21247896 | 48967; RRID:Addgene_48967 |
| PCX4-PURO HA-SUMO2 | This work | N/A |
| PCX4-PURO ATP6V0D2-FLAG | This work | N/A |
| Software and algorithms | | |
| Prism GraphPad Software | Prism | www.graphpad.com |
| FIJI | Schindelin et al., 2012. https://doi.org/10.1038/nmeth.2019 | fiji.sc |

## RESOURCE AVAILABILITY

### Lead contact

Further information and requests for resources and reagents should be directed to and will be fulfilled by the lead contact, Neal Silverman (Neal.Silverman@umassmed.edu).

### Materials availability

This study generated new unique reagents. The authors declare that all data supporting the findings of this study are available within the article and its supplemental information files or are available from the authors upon request.

### Data and code availability

- Data: All data supporting the findings of this study are available within the article or available from the corresponding author upon request.
- Code: This study did not generate any code.
- Other items: Any additional information required to reanalyze the data reported in this paper can be requested to the lead contact.

## EXPERIMENTAL MODEL AND SUBJECT DETAILS

### Ethics statement: Our lab conducted all experiments according to the guidelines of the American Association for Laboratory Animal Science and approved by the Institutional Animal Care and Use Committee at the University of Massachusetts Medical School (Docket#: A-2056-19).Drosophila SL2 cells

Schneider's Drosophila Line 2 (D. Mel. (2), SL2) was isolated from several hundred 20 to 24 hour *Drosophila melanogaster* embryo (Schneider, 1972) and distributed to several researchers worldwide. Cells were grown at 27°C in Schneiders Drosophila Medium supplemented with 10% Fetal Bovine Serum. Cell cultures were split 1:10 when they reached 80–100% of confluency.

### Mouse bone marrow derive macrophages (BMDM)

Mouse bone marrow derive macrophages were obtained from C57BL/6 and Balb/c mice (The Jackson Laboratory). Seven to twelve-week-old female mice were maintained under pathogen-free conditions at the University of Massachusetts Medical School animal facilities. Animals were euthanized, femurs and tibia were dissected, and the bone marrow was flushed with PBS using a 30G needle connected to a 10 mL syringe. The cells were cultivated in RPMI supplemented with 30% L929 cell-conditioned medium and 20% FBS in bacteriological petri dishes ($4 \times 10^6$ cells/plate) at 37°C and 5% $CO_2$ [67]. The cultures were re-fed on day 3 with the same media and maintained in RPMI supplemented with %5 L929 cell-conditioned medium and 10% FBS. BMDMS were used for in the experiments on day 7–10.

### Leishmania amazonensis

GFP-transfected *L. amazonensis* (MHOM/BR/1973/M2269), and dsRed-transfected (RAT/BA/LV78) (Dutta et al., 2005) were generously donated by Dr. Silvia R. Uliana (ICB-USP, Brazil) and Dr. Kwang-Poo Chang (Rosalind Franklin University of Medicine and Science), respectively. Promastigotes were cultivated

*in vitro* in M199 medium supplemented with 10% FBS and 5 μg/mL hemin. Parasites were selected with 30 μg/mL Hygromycin B (GFP transfected) or 5 μg/mL of Tunicamycin (dsRed transfected) in the culture media at 27°C. In all cases, amastigotes were harvested from infected BMDMs to be used in the experiments. To cultivate these amastigotes, first promastigote forms were differentiated axenically to amastigote by cultivating the parasites with 199 media supplemented with 0.25% glucose, 0.5% trypticase, 40 mM sodium succinate (pH 5.4) and 20% FBS, at 1 × 10^7 cells/mL at 34°C for 3 days. Axenic amastigotes were then used to infect Balb/c BMDM cultivated in 175 $cm^2$ T-flasks (3 × $10^7$ cells/flask) at a multiplicity of infection of 3 parasites/BMDM. Seven to 14 days after infection cells were harvested from T-flasks using a cells scraper and disrupted in PBS at 4°C using a glass dounce tissue grinder with teflon rod. Amastigotes were enriched by two-step centrifugations, one at 210*g* for 8 min to remove intact BMDMs and cell debris, and then supernatant was centrifuged at 675*g* for 12 min to precipitate amastigotes.

### THP-1

THP-1 (ATCC, TIB-202) is a human monocyte isolated from peripheral blood from an acute monocytic leukemia 1 yearold male patient. Cells were cultured in suspension in RPMI 10% FBS at 37°C and 5% $CO_2$ at concentrations of 3 × $10^5$ to $10^6$ cells/mL. THP-1 monocytes were differentiated to macrophages by stimulation with 100 ηg/mL of phorbol 12-myristate 13-acetate (PMA) in RPMI 10% FBS for 48 h, washed and cultured for additional 24 h in complete media without PMA, prior use.

### RAW 264.7

This cell line is derived from a male BALB/c mice. Cells were cultivated in DMEM supplemented with 10% FBS at 37°C and 5% $CO_2$ atmosphere. Cells were split 1:10 when the cultures reached 100% confluence.

## METHOD DETAILS

### Confocal microscopy

SL2 cells were seeded (2 × $10^5$ cells per dish) in 35 mm dish with glass bottom one day before infection. Cells were infected with amastigotes and at determined times, cell membranes were stained with CellMask deepRed for 10 min, and acidic organelles were stained with Lysotracker Blue DND-22 (Invitrogen). Confocal images were taken using a Leica SP8 confocal microscopy using a 63x objective. Images were edited using Fiji software (Schindelin et al., 2012).

### HTS screening

For genomewide screen a library of 13,071 dsRNA against *D. melanogaster* genes (Ambion Silencer Drosophila RNAi Library) distributed in 32 384-well plates with clear bottom (Costar) was utilized. SL2 cells were maintained in complete media (Schneider media (Gibco), 10% fetal bovine serum (Optima, Atlanta Biologicals), 100 U of penicillin and streptomycin) at 27°C. After changing to serum-free media, 20,000 cells in 10 μL of was added to each well, which contained 250 ηg dsRNA, and incubated for 1 h, then 20 μL of complete media was added per well and incubated for 72 h for knockdown. GFP expressing amastigotes harvested from BMDMs ($10^4$ in 5 μL of Schneider media per well) were added to each well and the plates centrifuged at 300 x G for 5 min and kept at 27°C for 90 min. The media was carefully removed from wells and cells were fixed with 20 μL of 3.2% formaldehyde (EM grade, EMS) for 30 min at room temperature and not permeabilized. The cultures were washed once with PBS and blocked with 1% bovine serum albumin (BSA) for 1 h at 37°C. Extracellular parasites were immunostained with serum of an infected Balb/c diluted 1:4000 in PBS with 1% BSA, and a secondary goat anti-mouse conjugated to Alexafluor 594 1:1000 (Invitrogen). The DNA of cells were counterstained using 0.1 μg/ml Hoechst 33342 added to the secondary antibody solution, the general scheme for the method is shown in Figure S2. Three fields per well, close to the center of wells, were imaged using a 20x objective using an ImageXpress Micro automated microscope and analyzed using MetaXpress software (Molecular Devices). Number of SL2 cells (Hoechst 33342 staining), total parasites (GFP positive), and extracellular parasites (GFP and AlexaFluor 594 positive), intracellular parasites (GFP positive and AlexaFluor 594 negative) were scored and averaged for the three images of each well. The infection rate (number of intracellular parasites per SL2 cells) was log-transformed, and the median and interquartile range were used to calculate a Z-score: (log10(%infection)-log10(median))/(IQR*0.74) for each plate (Zhang et al., 2006). The entire screen was performed in duplicate and wells with Robust Z-scores of infection $\geq$ 1.5 or $\leq$ −2.0 in both replicates were considered 'hits'. Knockdowns that reduced the SL2 numbers by −2 Z-scores received lower priority to further studies.

### dsRNA synthesis and secondary screen

Primer sequences to generate dsRNA sequences with no off-targets were obtained from DRSC/TRiP Functional Genomics Resources (www.flyrnai.org) or manually designed using SnapDragon (https://www.flyrnai.org/cgi-bin/RNAi_find_primers.pl) (see Table S2). After PCR using genomic DNA from flies, dsRNA was synthesized using MEGAscript T7 transcription kit (Invitrogen) following manufacturer recommendations.

The secondary screen plates were arrayed with dsRNA (250 ηg) using on-site synthesized dsRNA free of off targets. Genes were considered hits when two of the triplicates Robust Z-scores in infection was $\geq 1.5$ or $\leq 1.5$ using dsRNA against 180 wells treated with dsRNA against β-galactosidase.

### Phagocytosis of *E. coli* and *S. aureus*

SL2 cells were soaked with 1.25 μg of dsRNAs in 96 well plate for 3 days prior to phagocytosis assays. Fluorescein-labeled *E. coli* (K-12 strain), and *Staphylococcus aureus* (Wood strain, without protein A) (Invitrogen), were washed 3 times with PBS by centrifugation and sonicated for 3 times at 50 kHz for 20 s. Twenty micrograms of bacterial particles were added to each well at 4°C, the plates were centrifuged 300xg for 3 min at 4°C, and incubated in a 27°C water bath for 20 or 40 min (for *E. coli* and *S. aureus*, respectively). Cells and bacteria were removed from plates at 4°C by pipetting 300 μL of a 0.1% Trypan Blue solution in PBS pH 5.4 to quench the fluorescein from extracellular bacteria. The mount of bacteria inside live cells was quantified by flow cytometry (Ramet et al., 2002).

### Bioinformatic analysis

The clustering and enrichment analysis of the screen hits was performed in PANTHER Classification System (Thomas et al., 2003). The hits were submitted to PANTHER Overrepresentation Test (Released 20220202), using *Drosophila melanogaster* reference list and the PANTHER GO-Slim Biological Process. The raw p-value determined by Fisher's Exact test or Binomial statistics. Correction: False Discovery Rate by the Benjamini-Hochberg procedure. Fold Enrichment: number of genes observed in the uploaded list over the number of expected genes. If it is greater than 1, it indicates that the category is overrepresented in your experiment. Conversely, the category is underrepresented if it is less than 1.

### Macrophage transduction

SUMO1 and SUMO2 were knocked down using GIPZ lentiviral particles from GE Dharmacon V3LHS_404077 and V3LHS_412780. SUMO2 and ATP6V0D2 (NM_152565.1) was cloned with a C-terminus tag in the lentiviral vector PCX4-PURO and used to generate lentiviral particles and transduce macrophages. Cells were selected with puromycin for 3 days before use.

### Western blot

Macrophages were lysed in standard lysis buffer containing 10% glycerol, 1% Triton X-100, 20 mM Tris, 150 mM NaCl, 24 mM β-glycerol phosphate, 1 mM $MgCl_2$, 1 mM 1,4 dithiothreitol (DTT), 1 mM sodium orthovanadate, 5 mM N-ethylmaleimide, 0.5 U/μl Benzonase, 1× protease inhibitor mixture (Halt, Thermofisher). A 5 μL of lysate was reserved for protein quantification by Bradford protein assay (Bio-Rad). Laemmli SDS sample buffer with reducing agent was added to samples immediately after cell lysis and heated for 3 min at 95°C. For whole cell lysate analysis, 30 μg of total protein was separated by SDS-PAGE using 8% or 4–20% polyacrylamide gels, and transferred to PVDF membranes at 350 mA for 40 min using BioRad Mini Protean and Transblot system (Bio-Rad). Membranes were blocked with 5% non-fat dry milk for 1 h and probed with primary antibodies against SUMO1 or SUMO2/3 (Cell Signaling C9H1 and 18H8) 1:1000 dilution, anti-SAE1 (Thermo Scientific PA522297) 0.5 μg/mL, Anti-Ubc9 (BD Biosciences 610748) 0.5 μg/mL for 16 h at 4°C in a rotator. For loading controls, the same blots were with Coomassie blue.

### Production of retroviral vectors and transduction of immortalized mouse macrophages

The full length mouse SUMO2 fused to HA (N-terminus) from a plasmid (Addgene 48967) (Bekes et al., 2011) were inserted in the retroviral transfer plasmid pCX4 Puro. For the viral production, HEK 293T cells were transfected with the pCX4 HA-SUMO2, MLV gag-pol, and VSVG using GeneJuice transfection reagent (EMD Millipore) following the manufacturer's recommendations. Media was replaced at 24 h and collected 48 h after transfection, filtered through a 0.45 μm pore filter and stored at −80°C until use. Virus for shRNA transduction were generated using shRNA library (GIPZ, Dharmacon): SUMO2 (V3LHS_412780), SUMO1- (V3LHS_404077). THP-1 cells were cultured in the presence of virus particles and 8 μg/mL

Polybrene for 24 h, and then the transduced cells were selected with 3 μg/mL of puromycin for 4 days. Cells were frozen and when the thawed aliquots were subcultured for up to 3 weeks.

### ATP6V0D2 plasmid

Human ATP6V0D2-FLAG NM_152565.1 was obtained from Sino Biological (HG23801-CF) and cloned in PCX4-Puro lentiviral plasmid.

### Macrophage infection and PV area measurement

THP-1 macrophages were infected with amastigotes for 2 h and the coverslips were washed 3 times with RPMI media and transferred to a new plate. One day after infection the cultures were fixed with 4% paraformaldehyde for 15 min and mounted over a glass slide for microscopic imaging in a fluorescence microscope. The area of PVs containing 1 or 2 parasites was manually measured using an elliptical tool in FIJI.

### Cholesterol localization using filipin staining

RAW 264.7 macrophages were cultivated in 96 well plate with optical bottom (Falcon 353219) (30,000 cells/well) overnight, infected with amastigotes with MOI = 2 for 1 h, washed to remove free parasites and after 6 h of interaction amastigote/macrophage the culures were fixed with 4% paraformaldehyde for 30 min and permeabilized for 10 min with 0.1% Triton X-100/PBS. Cholesterol and DNA staining was performed with PBS/10% FCS containing 0.05 mg mL−1 filipin (F9765 Sigma-Aldrich, St. Louis, USA) and 1 μg/mL Hoechst 33342 for 1 h at RT. Four fields per well, close to the center of wells, were imaged using a 4x objective using an LionHeart (Agilent Biotek) automated microscope and analyzed using Gen5 software. Macrophage nuclei were identified by Hoechst 33342 staining and intracellular amastigotes identified by GFP signal (GFP expressing *L. amazonensis*). The filipin fluorescence intensity was measured in the parasite/PV area including 5 μm surrounding the amastigotes.

### RNA and qRT–PCR

Total RNA from macrophages were isolated using the TRIzol reagent (Invitrogen) following the manufacturer's recommendations. cDNA was synthesized using iScript gDNA Clear cDNA synthesis kit (BioRad) and quantitative PCR analysis was performed using SYBR Green (BioRad). The specificity of amplification was assessed for each sample by melting curve analysis and relative quantification was performed using a standard curve with dilutions of a standard. The oligonucleotides used qPCR reactions are listed in the Table S2.

### Cholesterol measurement

Macrophages were seeded in 96 well plates (5 × 10^4 cells per well), one day later free and total cholesterol in lysates was determined using Cholesterol/Cholesterol Ester-Glo Assay (Promega) following manufacturer recommendations. The concentration of cholesterol was normalized by the protein concentration of cells cultured in parallel determined using Bio-Rad Protein Assay Dye (Bio-Rad).

## QUANTIFICATION AND STATISTICAL ANALYSIS

The statistical analyses were performed using GraphPad Prism version 6.00 for Mac OS X, GraphPad Software, La Jolla California USA, www.graphpad.com. A p value of $<0.05$ was considered statistically significant. The exact value of n and the statistical method used for each comparison within the figures is indicated in the figure legends.